© Entomological Society of Indochina
អ្នកជំនាញខាងជាណកសាស្ត្រឥណ្ឌូចិន
The Indochina Entomologist
OPEN ACCESS
Genetics
ICE, 1 (63): 593–609 (2025)
ISSN (Online) 3065-1107
www.indochinaentomologist.com

https://doi.org/10.70590/ice.2025.01.63
http://zoobank.org/urn:lsid:zoobank.org:pub:F89A9E3E-A8E8-47C8-BEBD-78844EBCED3C

Genetic diversity and population structure of *Diaphorina citri* (Hemiptera: Liviidae) in Sichuan Province, China

Hong-Ling LIU[1], Yan-Ping WANG[2], Song CHEN[3], Cui-Cui ZHANG[4], Qing-Dong CHEN[5], Chun-Yan YI[6], Xu LIU[7] & Mao WANG[8*]

Institute of Plant Protection, Sichuan Academy of Agricultural Sciences, Key Laboratory of Integrated Pest Management of Southwest Crops, Ministry of Agriculture, Chengdu 610066, China

[1] https://orcid.org/0000-0001-7960-009X; liuhongling1972@outlook.com
[2] https://orcid.org/0009-0005-5947-7959; singular2023@outlook.com
[3] https://orcid.org/0009-0006-4044-1857; chensong523@126.com
[4] https://orcid.org/0009-0002-8066-9822; zhangcuicui@scsaas.cn
[5] https://orcid.org/0009-0000-8433-1402; chenqingdong03@outlook.com
[6] https://orcid.org/0009-0008-1476-3996; yichunyan2022@163.com
[7] https://orcid.org/0009-0002-3989-8623; liuxu6186@126.com
[8] https://orcid.org/0000-0001-9322-334X; maode2046@163.com
*Corresponding author

Abstract: *Diaphorina citri* Kuwayama (1908), the Asian citrus psyllid (ACP), is a major pest of citrus crops, responsible for transmitting the bacterium that causes Huanglongbing (HLB), a disease devastating to citrus industries worldwide. Despite extensive research on its population genetics in other regions, the genetic structure of *D. citri* in Sichuan Province, China, remains poorly understood, complicating the development of effective pest management strategies. This study aims to fill this gap by investigating the genetic diversity and population structure of *D. citri* using genome-wide single nucleotide polymorphisms (SNPs). Three natural populations of *D. citri* from southeastern Sichuan were sequenced, revealing a total of 7,010,305 SNPs and relatively low genetic differentiation among populations. Phylogenetic analysis identified two primary genetic groups with limited gene flow, supported by principal component analysis (PCA) and Admixture analysis. The populations exhibited high genetic diversity, with notable variations in nucleotide diversity and inbreeding coefficients. Functional enrichment analysis highlighted genes involved in cellular processes and stress response, which may contribute to local adaptation. These findings provide valuable insights into the evolutionary dynamics of *D. citri* and suggest that genetic diversity and selective pressures play a key role in its adaptability. The results underscore the importance of considering genetic variation in the development of targeted and sustainable pest management strategies in southeastern China.

Keywords: Genetic differentiation, Phylogeography, Population genetics, Population history, Whole-genome sequencing

四川省柑橘木虱（半翅目：扁木虱科）的遗传多样性与种群结构

刘虹伶，王燕平，陈松，张翠翠，陈庆东，易春燕，刘旭 & 王毛*

四川省农业科学院植物保护研究所/农业部西南作物有害生物综合治理重点实验室，成都 610066，中国
*通讯作者

Accepted by Cheng-Bin WANG: 2.IX.2025; published online: 4.IX.2025

Copyright Hong-Ling LIU *et al*. This is an open access article distributed under the terms of the Creative Commons Attribution License (CCBY 4.0), which permits unrestricted use, distribution, and reproduction in any medium, provided the original author and source are credited.

摘要：柑橘木虱 *Diaphorina citri* Kuwayama, 1908 是柑橘作物的主要害虫，负责传播引起黄龙病（Huanglongbing, HLB）的病原细菌，该病对全球柑橘产业造成毁灭性打击。尽管在其他区域对其种群遗传学已有广泛研究，但中国四川省柑橘木虱的遗传结构仍知之甚少，这阻碍了有效害虫管理策略的制定。本研究旨在利用全基因组单核苷酸多态性（SNPs）技术，调查四川省柑橘木虱的遗传多样性与种群结构，以填补这一空白。对来自四川省东南部的三个自然种群进行了测序，共检测到 7,010,305 个 SNPs，种群间遗传分化程度相对较低。系统发育分析、主成分分析（PCA）和 Admixture 分析支持存在两个主要的遗传类群，且基因流有限。种群表现出较高的遗传多样性，核苷酸多样性和近交系数存在显著变异。功能富集分析强调了涉及细胞过程和胁迫响应的基因，这些基因可能有助于本地适应。这些发现为理解柑橘木虱的进化动态提供了有价值的见解，表明遗传多样性和选择压力在其适应性中起着关键作用。研究结果强调了在制定中国东南部靶向和可持续害虫管理策略时，考虑遗传变异的重要性。

关键词：遗传分化，系统地理学，群体遗传学，种群历史，全基因组测序

Citation: Liu H-L, Wang Y-P, Chen S, Zhang C-C, Chen Q-D, Yi C-Y, Liu X & Wang M 2025: Genetic diversity and population structure of *Diaphorina citri* (Hemiptera: Liviidae) in Sichuan Province, China. *The Indochina Entomologist*, 1 (63): 593–609. [刘虹伶, 王燕平, 陈松, 张翠翠, 陈庆东, 易春燕, 刘旭 & 王毛 2025: 四川省柑橘木虱（半翅目：扁木虱科）的遗传多样性与种群结构. 中南半岛昆虫学家, 1 (63): 593–609.]
https://doi.org/10.70590/ice.2025.01.63

Introduction

Diaphorina citri Kuwayama (1908), commonly known as the Asian citrus psyllid (ACP), is a small but highly impactful insect in the agricultural sector, particularly in citrus-producing regions (Hall *et al.* 2013; Du *et al.* 2023). As a member of the hemipteran family Liviidae, *D. citri* is the primary vector of the bacterium responsible for the devastating citrus disease Huanglongbing (HLB), also known as citrus greening disease (Grafton-Cardwell *et al.* 2013). The feeding behavior of *D. citri* facilitates the introduction of the pathogen into the phloem of citrus plants, resulting in substantial economic losses due to reduced fruit quality and tree mortality. Globally, *D. citri* is recognized as one of the most destructive pests of citrus crops, prompting extensive studies into its biology, ecology, and population dynamics, all of which play a significant role in managing its spread and impact on citrus industries worldwide (Zheng *et al.* 2018). In addition to its role as a vector, the species' adaptive biology has enabled its rapid spread to numerous citrus-growing regions, including the recent invasion to southeastern Sichuan, China, where it poses a significant threat to both domestic citrus production and the broader agricultural economy (Huang *et al.* 2024).

While much of the previous research on the population structure and genetic diversity of *D. citri* has focused on various areas (Guidolin *et al.* 2014; Lashkari *et al.* 2014; Fuentes *et al.* 2018; Qasim *et al.* 2018; Song *et al.* 2018; Luo *et al.* 2019; Pérez-Valencia *et al.* 2019; Ajene *et al.* 2022; Deng *et al.* 2024; Huang *et al.* 2024), there are notable gaps in our understanding, especially in key citrus-producing areas such as Sichuan Province of China. Consequently, the genetic structure of *D. citri* in Sichuan Province remains poorly understood, which complicates the development of region-specific pest management strategies.

This study aims to bridge these gaps by investigating the genetic diversity and population structure of *D. citri* in southeastern Sichuan Province, where they invaded in recent years. Using genome-wide single nucleotide polymorphisms (SNPs), this research provides a detailed examination of the genetic diversity and population structure within local populations. The findings offer new insights into the phylogeography and genetic composition of *D. citri* in this region, contributing valuable information that will help inform targeted and sustainable pest management strategies to combat both *D. citri* and the spread of HLB in southwestern China.

Material and methods

Sampling and sequencing

In this study, three natural populations of *D. citri* were collected from southeast Sichuan Province, China. Each population consisted of 10 individuals, resulting in a total of 30 samples (Table 1). Genomic DNA was extracted from muscle tissue using the TIANGEN Blood & Tissue Kit (Tiangen, Beijing, China), following the manufacturer's protocol. DNA quality was assessed using 0.8% agarose gel electrophoresis, and the DNA concentration was quantified with a UV spectrophotometer (Thermo Fisher Scientific, Waltham, MA, USA).

Table 1. Information of samples used in this study.

Group name	Sample name	Longitude	Latitude	Location
popA	sam1	104°30′23″E	28°47′3″N	Yibin City, Cuiping District, Sipo Town, Xiaolong Village, Group 4
popA	sam2	104°34′42″E	28°47′27″N	Yibin City, Cuiping District, Zongchang Town, Hefu Community, Group 4
popA	sam3	104°35′47″E	28°45′27″N	Yibin City, Cuiping District, Xijiao Street, Jianxin Village
popA	sam4	104°30'22"E	28°47'2"N	Yibin City, Cuiping District, Sipo Town, Xiaolong Village
popA	sam5	104°34'43"E	28°47'27"N	Yibin City, Cuiping District, Caiba Town, Shima Village
popA	sam6	103°50′58″E	28°24′12″N	Liangshan Prefecture, Leibo County, Dukou Town, Xiaba Village, Group 3
popA	sam7	103°29′47″E	28°9′10″N	Liangshan Prefecture, Leibo County, Qiannian Guan Township, Shibanpan Village
popA	sam8	103°41′32″E	28°15′16″N	Liangshan Prefecture, Leibo County, Yongsheng Town, Quli Mi Village
popA	sam9	103°19′5″E	28°3′9″N	Liangshan Prefecture, Leibo County, Mohong Township, Qiantuo Village, Group 2
popA	sam10	103°26′55″E	28°6′17″N	Liangshan Prefecture, Leibo County, Shangtianba Town, Shangxingzhai Village
popB	sam11	104°39′0″E	30°45′2″N	Chengdu City, Jintang County, Sanxi Street, Jinfeng Village
popB	sam12	103°34'29"E	30°23'42"N	Chengdu City, Qionglai City, Guyi Street, Linshan Village
popB	sam13	104°25'28.022"E	30°57'23.905"N	Deyang City, Guanghan City, Lianshan Town, Jingjin Highway
popB	sam14	103°55′8″E	30°7′4″N	Meishan City, Dongpo District, Funu Town, Changhong Community
popB	sam15	103°23′27″E	29°59′36″N	Meishan City, Danleng County, Renmei Town, Guixiang Village
popB	sam16	104.100037°E	30.244296°N	Chengdu City, Shuangliu District, Jitian Street, Xiaoyangou Village, Group 6, No. 62
popB	sam17	103°55′8″E	30°6′57″N	Meishan City, Dongpo District, Funu Town, Changhong Community (repeated)
popB	sam18	104°37'42.99"E	29°59'20.29"N	Ziyang City, Yanjiang District, Fengyu Town, Xinhua Village
popB	sam19	104°40'32.09"E	30°10'44.95"N	Ziyang City, Yanjiang District, Linjiang Town, Kunlun Village
popB	sam20	104°41'13.55"E	30°15'36.98"N	Ziyang City, Yanjiang District, Laojun Town, Quanxi Village
popC	sam21	105°41′54″E	27°43′32″N	Luzhou City, Gulin County, Maiti Town, Nabao Village, Group 5
popC	sam22	106°8′1″E	28°4′23″N	Luzhou City, Gulin County, Dongxin Town, Xingwen Village
popC	sam23	106°8′16″E	28°5′8″N	Luzhou City, Gulin County, Erlang Town, Wenming Village
popC	sam24	104°5′41″E	29°28′30″N	Zigong City, Rong County, Liu Jia Town, Dawu Village
popC	sam25	104°36'7.52″E	29°47'49.86″N	Neijiang City, Zizhong County, Tiejie Town, Guihua Village
popC	sam26	104°17'0.57"E	29°39'0.51"N	Neijiang City, Weiyuan County, Xiaohui Town, Paifang Village
popC	sam27	104°6'44.59″E	29°42'19.23″N	Leshan City, Jingyan County, Jiyi Town, Fansheng Fruit Industry
popC	sam28	104°2'35.35"E	29°23'54.70"N	Leshan City, Qianwei County, Luocheng Town, Datong Village
popC	sam29	104°4′54″E	29°35′35″N	Leshan City, Jingyan County, Qianfo Town, Minjian Village
popC	sam30	104.1579°E	29.6589°N	Leshan City, Jingyan County, Donglin Town, Dagutan Village

For sequencing, paired-end libraries with a 400 bp insert size were prepared for each sample using the Illumina TruSeq DNA PCR-free preparation kit (Illumina Inc., San Diego, CA, USA) in accordance with the manufacturer's instructions. Prior to sequencing, library quality was verified on an Agilent 2100 Bioanalyzer (Agilent Technologies, Santa Clara, CA, USA) with the Agilent High Sensitivity DNA Kit, and library concentration was measured using the Promega QuantiFluor fluorescence quantitative system with the Quant-iT PicoGreen dsDNA Assay Kit (Thermo Fisher Scientific, Waltham, MA, USA).

Sequencing was performed on the Illumina NovaSeq platform (Illumina, San Diego, CA, USA) at Shanghai Personal Biotechnology Co., Ltd. (Shanghai, China) using paired-end reads of 2 × 150 bp.

Sequence mapping and SNP calling

Raw Illumina reads were filtered for quality control using Fastp (v0.20.0) (Chen *et al.* 2018). High-quality reads were aligned to the *D. citri* reference genome (GenBank accession number GCA_000475195.1) using BWA-MEM (version 0.7.12-r1039) with default parameters (Li 2013). Sequencing data were processed by sorting and removing duplicates with Picard software v1.107 (http://broadinstitute.github.io/picard).

To improve the accuracy of SNP predictions, reads near insertion-deletion (InDel) events were realigned using the IndelRealigner tool from the Genome Analysis Toolkit (GATK) v3.8 (McKenna *et al.* 2010). SNPs were called using the Unified Genotyper module in GATK, and SNP sites were subsequently annotated using ANNOVAR software v2019Oct24 (Wang *et al*. 2010).

InDel detection and annotation

InDel sites were identified using the Unified Genotyper program in GATK v3.8. Parameters for the analysis included a minimum confidence threshold of 30 (stand_call_conf) and a minimum emission threshold of 10 (stand_emit_conf). The SelectVariants command was used to extract InDel mutation information, which was then annotated using ANNOVAR v2019Oct24.

Phylogenetic analysis

A phylogenetic tree based on SNP data was constructed using the Maximum Likelihood algorithm in FastTree (Price *et al.* 2009). This analysis provided insights into the evolutionary relationships among the 30 *D. citri* individuals and measured genetic distances between them.

To estimate genetic relationships, a genome-wide relationship matrix (G matrix) was computed, utilizing SNP data to quantify pairwise genetic distances between individuals using the Gmatrix v2 (VanRaden 2008). The Identical By State (IBS) similarity coefficient, which reflects the proportion of alleles shared between individuals, was calculated using PLINK v1.9 (Purcell *et al.* 2007). A distance matrix was generated by applying the formula 1 - IBS to compute pairwise genetic similarity.

Principal component analysis

Principal component analysis (PCA) was conducted to evaluate the genetic structure of *D. citri* populations using SNP data (excluding those with a minor allele frequency [MAF] < 0.05). PCA was performed using GCTA software v1.93.2 (Yang *et al.* 2011). Individuals were clustered into distinct subgroups based on their principal component values, enabling visualization of population structure.

Population genetic structure analysis

The Admixture software v1.3.0 (Alexander *et al*. 2009) was employed to analyze the genetic structure of the three *D. citri* populations based on SNP data. A mixed model was applied, with the number of ancestral populations (K) varied from 2 to 10, and the remaining parameters set to default values. The optimal K value was determined by minimizing the cross-validation (CV) error rates.

Gene flow analysis

Gene flow between populations was inferred using Treemix v1.13 (Pickrell & Pritchard 2012), which models population splitting and migration events based on genome-wide allele frequency data. The analysis was performed for 0 to 10 migration events using the -m parameter. The best-fit model was selected based on residual values, and the population maximum likelihood tree was constructed with migration events represented on the tree.

Linkage disequilibrium analysis

Linkage disequilibrium (LD) measures the non-random association of alleles at different loci and can reveal historical recombination events. To assess LD decay, the r^2 coefficient between pairwise SNPs within a 1,000 kb window was calculated using PopLDdecay software v3.40 (Zhang *et al.* 2019).

Population genetic diversity analysis

Genetic diversity within each population was assessed using the Populations program in the Stacks v1.4.8 package (Catchen *et al*. 2013). This included calculating F_{st} statistics and genetic diversity measures such as observed heterozygosity (H_o), expected heterozygosity (H_e), nucleotide diversity (π), and the inbreeding coefficient (F_{IS}). Additionally, Tajima's *D* analysis, which tests for deviations from neutrality, was conducted for each chromosome of the *D. citri* genome using the PopGenome package in R v3.2.3 (Pfeifer *et al.* 2014).

Selective sweep and gene function enrichment analysis

Regions of the *D. citri* genome that may have undergone selective sweeps were identified based on the distribution of nucleotide diversity (θ_π) and F_{st} statistics. Selection sweeps were defined by examining the 5% left and right tails of the θ_π distribution and the top 5% of F_{st} statistics. These regions were considered potential targets of selection.

Functional enrichment analysis of genes within these selection sweep regions was conducted using Gene Ontology (GO) and Kyoto Encyclopedia of Genes and Genomes (KEGG) annotations via DAVID v6.8 (Huang *et al.* 2009). This analysis helped identify potential biological processes and pathways that may have been influenced by selective pressure.

Results

SNP and InDel analysis

A total of 30 *D. citri* individuals from three populations were subjected to whole-genome sequencing. The numbers of raw sequencing reads per sample ranged from 31,474,504 to 80,429,978. After quality control, the number of high-quality reads per sample ranged from 30,919,594 to 78,414,392, and the sequencing depth varied between 8.87× and 22.45×. Overall, 7,010,305 SNPs were detected across the three populations of *D. citri* (Table 2). Base bias analysis revealed no significant preference for any particular base (Fig. 1A), both before and after SNPs. The mutation spectrum analysis classified SNPs into six distinct types (Fig. 1B), with T:A > C:G and C:G > T:A as the dominant substitution types.

InDel analysis identified insertion and deletion events in the genome (Table 3). The number of insertions ranged from 319,338 to 737,830, while deletions ranged from 219,615 to 591,244 across individuals. In general, shorter InDels occurred more frequently than longer ones (Fig. 1C). Notably, 63% of the InDel sites were located in exonic regions.

Table 2. SNP annotation statistics of *Diaphorina citri*.

Type	Number	Percentage
exonic total	270852	3.86
synonymous SNV	180837	2.58
nonsynonymous SNV	88435	1.26
stopgain	1235	0.02
stoploss	345	0
unknown	0	0
splicing	1256	0.02
ncRNA total	0	0
ncRNA_exonic	0	0
ncRNA_splicing	0	0
ncRNA_exonic;splicing	0	0
ncRNA_intronic	0	0
intronic	1759539	25.1
intergenic	4213050	60.1
UTR 5’	75439	1.08
UTR 3’	201393	2.87
UTR 5’; UTR3’	997	0.01
upstream	238660	3.4
downstream	229636	3.28
upstream; downstream	19483	0.28
Total	7010305	100

Table 3. InDel annotation statistics of *Diaphorina citri*.

Type	Number	Percentage
exonic total	13530	0.63
frameshift deletion	2662	0.12
frameshift insertion	4115	0.19
nonframeshift deletion	3653	0.17
nonframeshift insertion	2745	0.13
nonframeshift substitution	0	0
stopgain	291	0.01
stoploss	64	0
unknown	0	0
splicing	913	0.04
ncRNA total	0	0
ncRNA_exonic	0	0
ncRNA_exonic; splicing	0	0
ncRNA_splicing	0	0
ncRNA_intronic	0	0
ncRNA_UTR5	0	0
intronic	508507	23.84
intergenic	1363545	63.91
UTR 5’	27139	1.27
UTR 3’	58802	2.76
UTR 5’; UTR3’	298	0.01
upstream	81789	3.83
downstream	71898	3.37
upstream; downstream	6994	0.33
Total	2133415	100

Population Genetic Structure

The phylogenetic tree constructed using genomic SNPs indicated that the three populations were not genetically isolated (Fig. 2A). While the majority of individuals from population A (popA) clustered into a distinct clade, individuals from populations B (popB) and C (popC) were intermixed across multiple clades. This clustering pattern was further corroborated by the G matrix (Fig. 2B), IBS (Fig. 2C), and PCA analysis (Fig. 2D).

The Admixture analysis revealed that the optimal number of genetic clusters (K) was 2, as determined by the minimum CV error (Fig. 3A). This shows that the populations of *D. citri* in southeastern Sichuan can be divided into two major genetic groups (Fig. 3B). Specifically, samples 1–4 from popA appear to have diverged from a common ancestor (designated as ancestor I), while samples 11–20 from popB and samples 24–30 from popC appear to share a separate ancestry (ancestor II). The remaining samples (5–10 from popA and 21–23 from popC) exhibit evidence of hybridization, likely representing admixture between ancestors I and II. This genetic structure was also supported by PCA, which showed clear separation between the two genetic groups.

Despite the observed genetic structure, the Treemix analysis did not provide clear evidence of gene flow between populations A, B, and C. The linkage disequilibrium (LD) analysis revealed that population C (popC) exhibited a significantly higher LD compared to populations A and B (Fig. 3C).

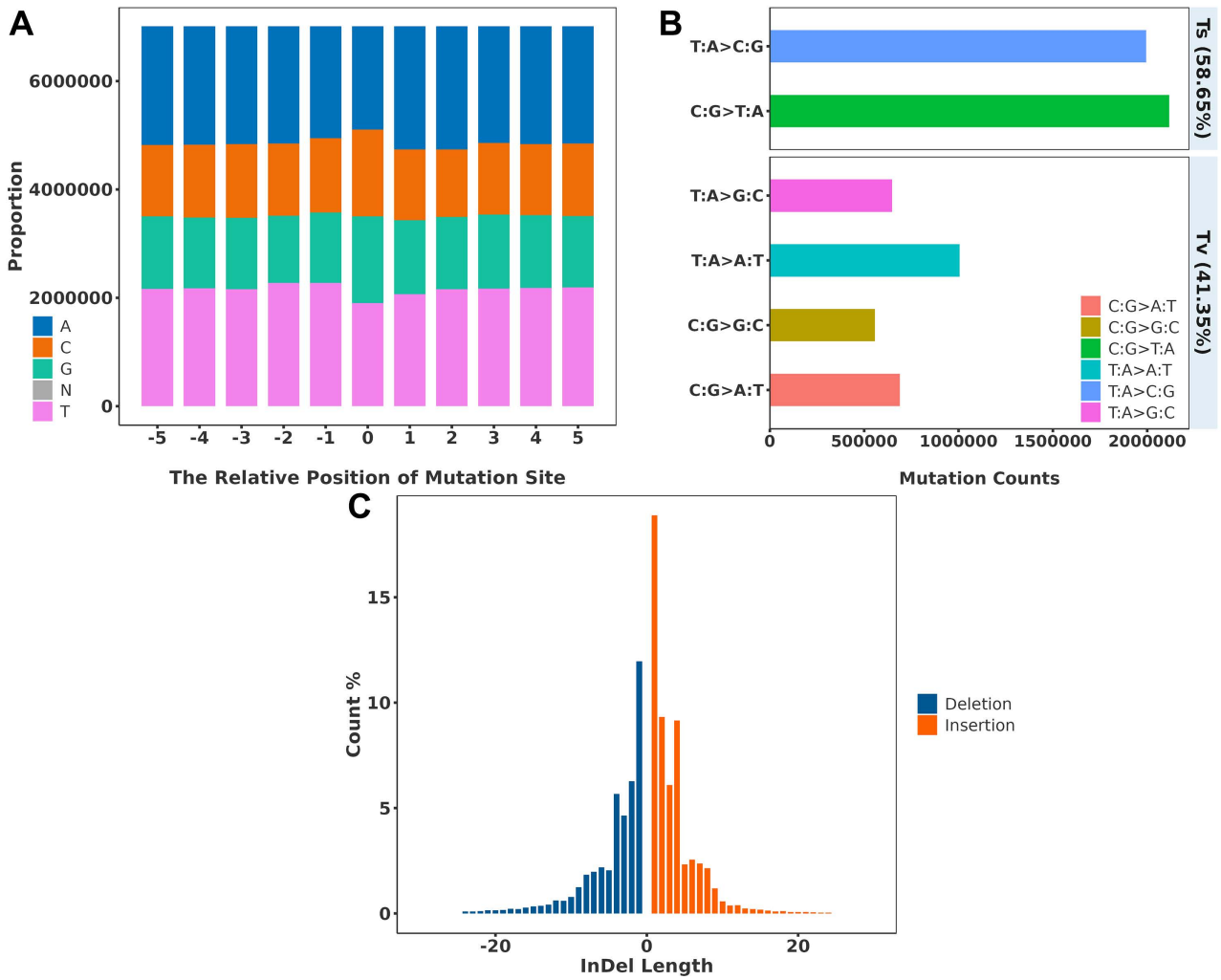

FIGURE 1. SNP and InDel information of *Diaphorina citri*: **A** base bias near SNPs **B** mutation spectrum of SNPs **C** distribution of InDel length.

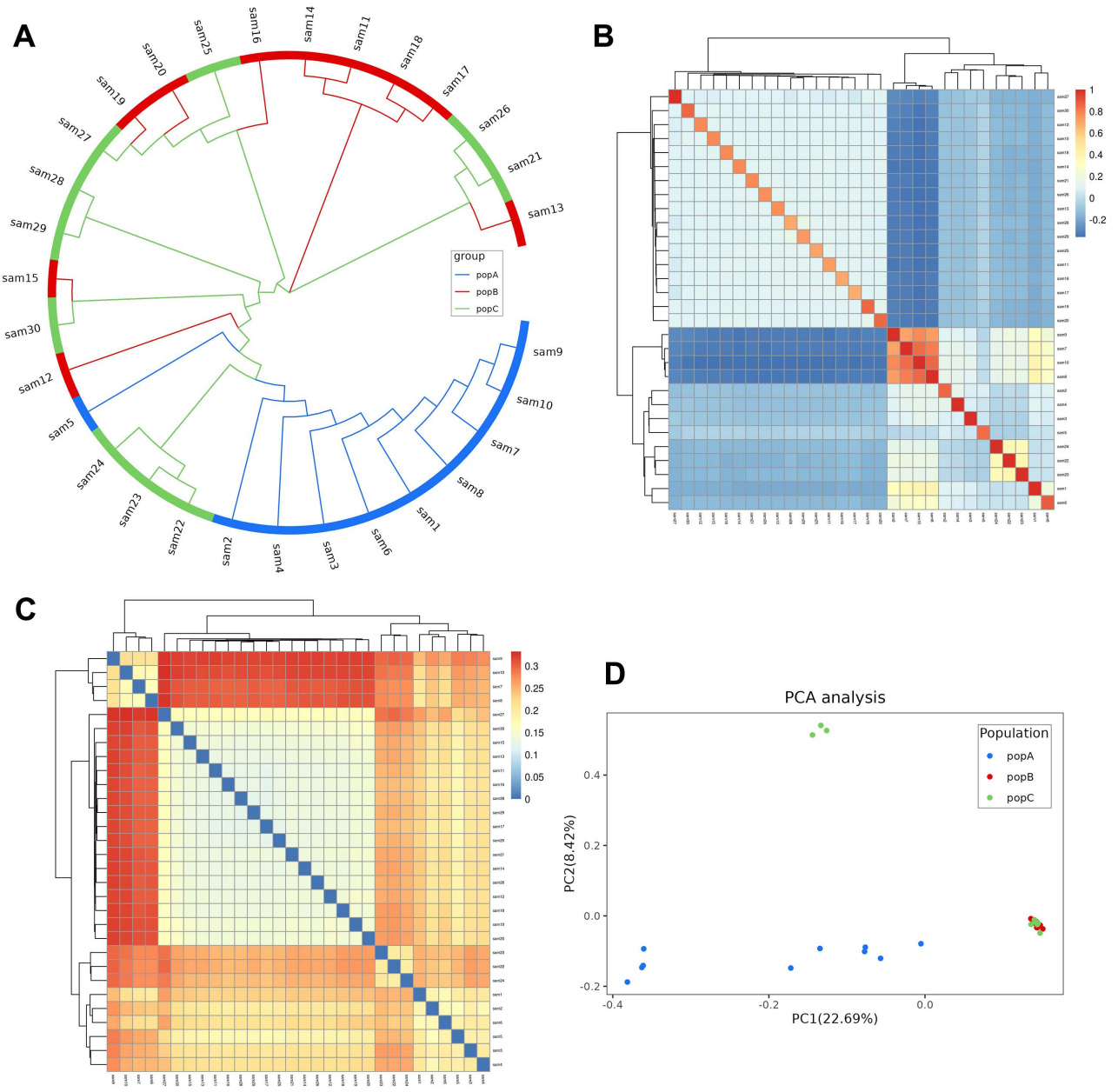

FIGURE 2. Relationships among samples of *Diaphorina citri*: **A** maximum likelihood tree of 30 individuals based on SNP data **B** Gmatrix heatmap **C** IBS heatmap **D** PCA analysis of the 30 individuals.

Genetic diversity patterns

The observed heterozygosity (H_o) was higher than the expected heterozygosity (H_e) across all populations (Table 4). Nucleotide diversity (π) was highest in popA (π = 0.353), followed by popC (π = 0.2957), and lowest in popB (π = 0.2214). Inbreeding coefficients (F_{IS}) were negative for all populations. The F_{st} statistics, which measure genetic differentiation among populations, were relatively low between popB and popC (F_{st} = 0.0389). However, F_{st} statistics were moderate between popA and popC (F_{st} = 0.0755) and higher between popA and popB (F_{st} = 0.1061). Tajima's *D* analysis revealed mostly positive values across all chromosomes in all populations of *D. citri* (Fig. 4).

Table 4. Population genetic diversity statistics of *Diaphorina citri*.

Pop ID	Individual number	H_o	O_h	H_e	E_h	π	F_{IS}
popA	9.2508	0.3898	0.6102	0.3332	0.6668	0.353	-0.0686
popB	9.2363	0.2545	0.7455	0.2093	0.7907	0.2214	-0.0618
popC	9.2706	0.3224	0.6776	0.2794	0.7206	0.2957	-0.0456

Selective sweep and gene function enrichment

To identify regions potentially under selection, we combined the F_{st} statistics and nucleotide diversity (θ_π) indices (Fig. 5). The analysis revealed that more candidate regions were under selection in popA compared to popB and popC.

The GO annotations (Fig. 6A) of the selected regions indicated significant enrichment in cellular components such as the cytosol, molecular functions like octopamine receptor activity, and biological processes related to cytokine receptor binding. KEGG pathway enrichment analysis (Fig. 6B) identified significant associations with endocrine and calcium reabsorption pathways.

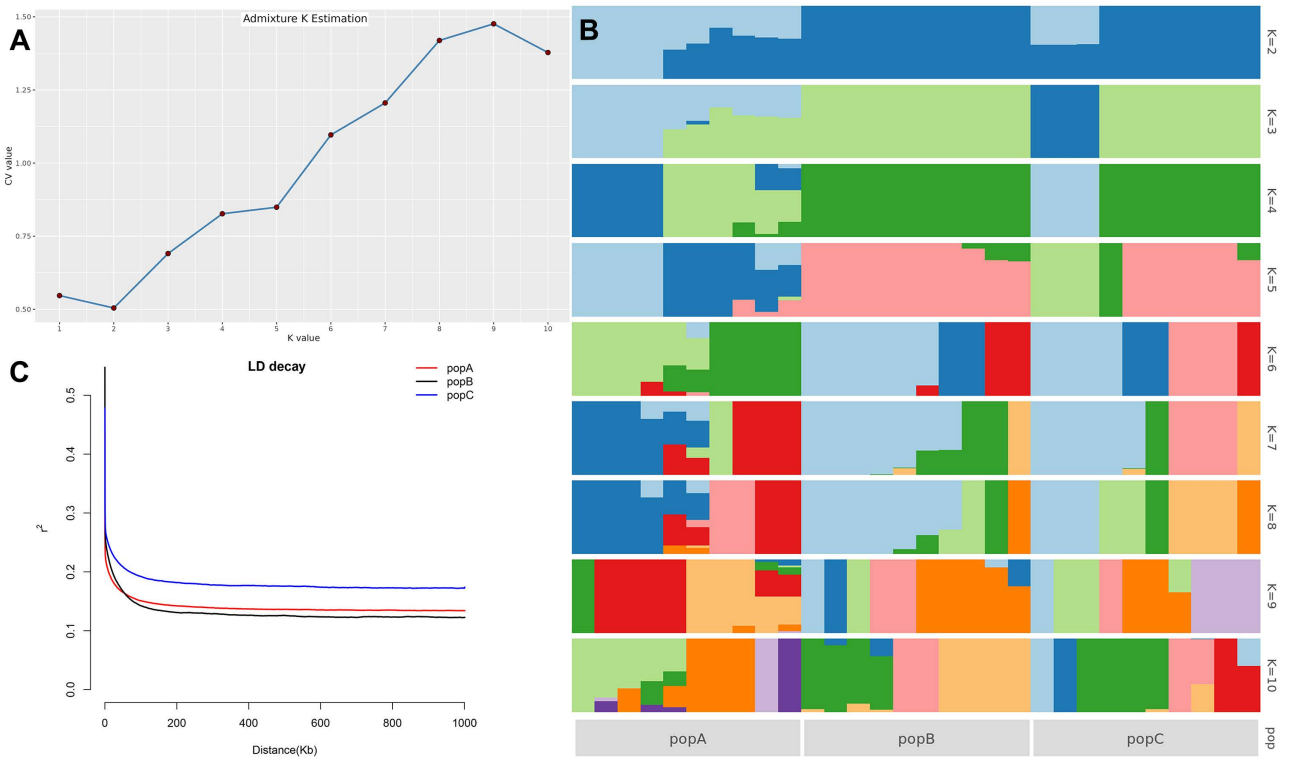

FIGURE 3. Population genetic structure: **A** Admixture K estimation curve **B** Population genetic structure of three populations **C** Linkage disequilibrium analysis of three populations.

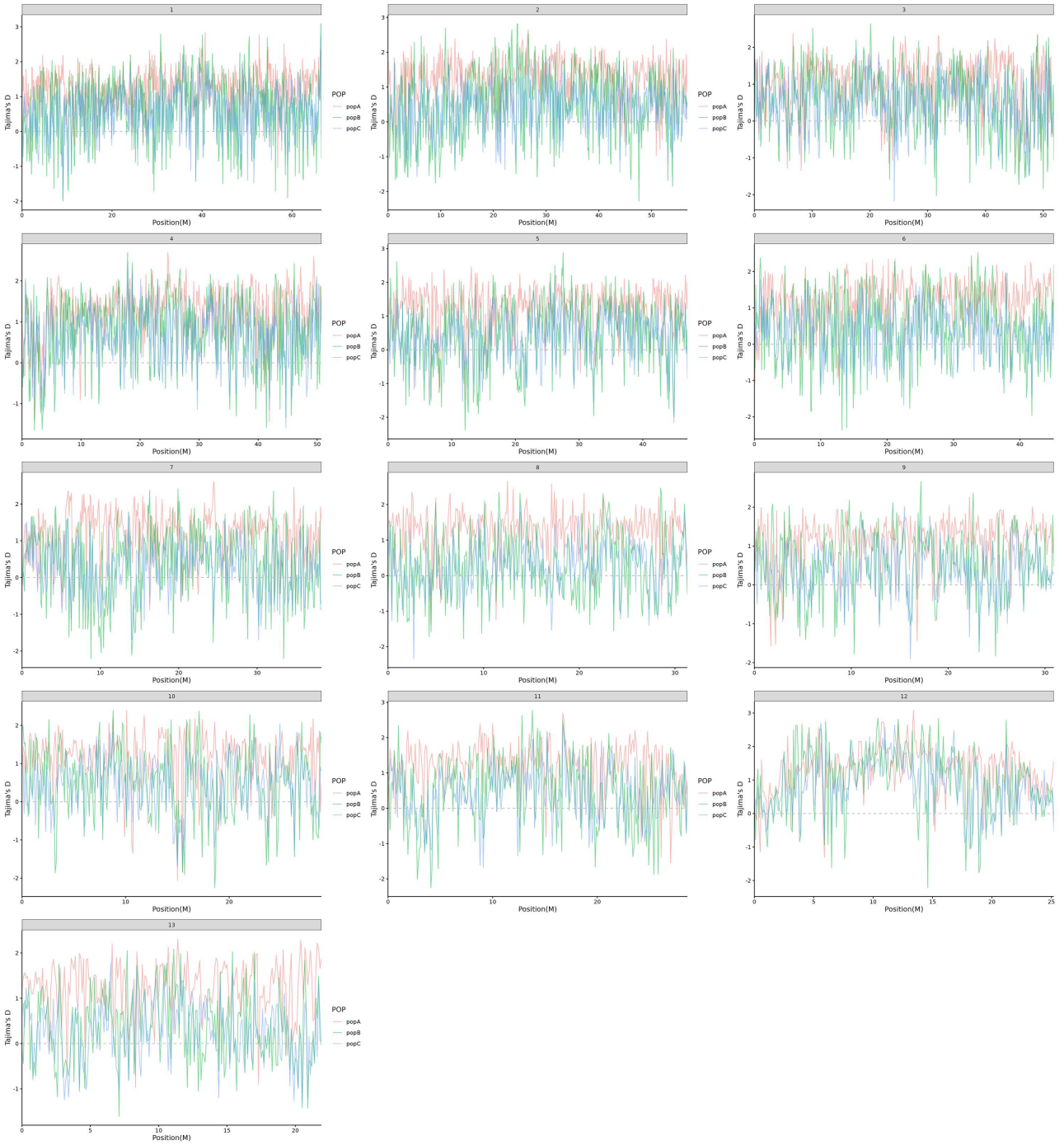

FIGURE 4. Tajima's *D* values of 13 chromosomes in populations of *Diaphorina citri*.

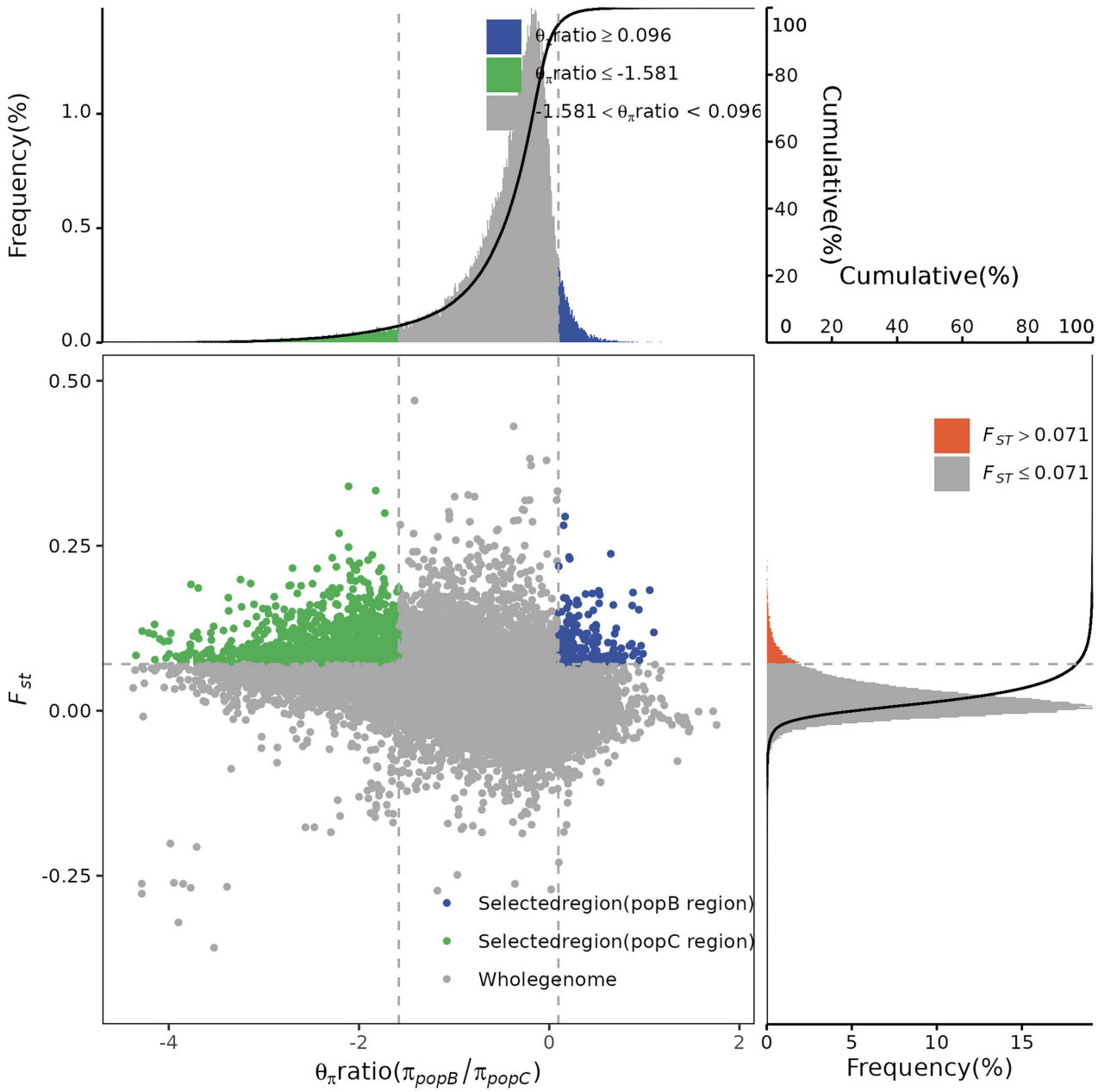

FIGURE 5. Combination F_{st} and θ_π analysis of *Diaphorina citri* using SNPs. The x-axis shows the value of the θ_π ratio, and the y-axis shows the F_{st} value, which correspond to the above frequency distribution diagram and the frequency distribution diagram on the right. The middle dot plots represent the corresponding F_{st} and θ_π ratio values in different windows. The blue and green regions are the top 5% regions selected by θ_π, and the red regions are the top 5% regions selected by F_{st}, while grey regions are unselected regions.

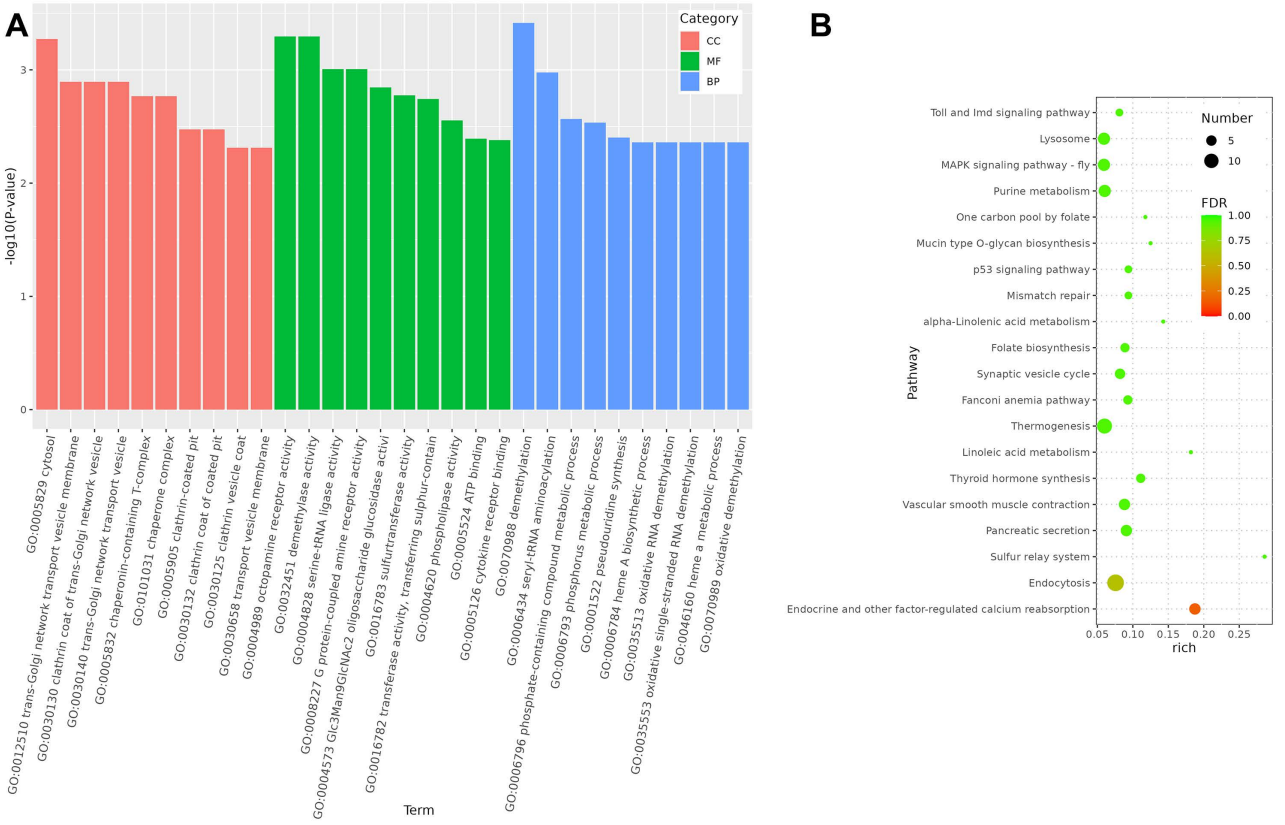

FIGURE 6. GO (**A**) and KEGG (**B**) enrichment analysis of *Diaphorina citri*.

Discussion

This study provides novel insights into the genetic diversity and population structure of *D. citri* in southeastern Sichuan Province, China. Based on whole-genome sequencing, our analysis reveals relatively low genetic differentiation among three populations of *D. citri*, with the identification of two primary genetic groups, which corresponds with the classification in previous studies (Wang *et al.* 2017; Zhang *et al.* 2019). These groups show evidence of historical separation and limited gene flow, likely influenced by geographical barriers or ecological preferences. The limited gene flow was also detected in other *D. citri* populations (Luo & Agnarsson 2018).

The phylogenetic tree and population structure analyses indicated that while the majority of individuals from popA clustered into a distinct clade, individuals from popB and popC intermixed across multiple clades, suggesting genetic admixture. This clustering pattern was further corroborated by the G matrix, IBS, and PCA analysis, which all showed relatively low genetic differentiation among the populations. The Admixture analysis, which identified two major genetic clusters, supports the existence of moderate genetic isolation between populations, with limited gene flow. Interestingly, Treemix analysis did not provide clear evidence of gene flow between populations A, B, and C, suggesting that migration between these populations may be limited. Additionally, LD analysis revealed that popC exhibited a significantly higher LD compared to popA and popB, which could indicate a more tightly linked genetic structure within popC.

The highest genetic diversity was observed in popA, followed by popC and popB, with nucleotide diversity and heterozygosity values supporting this trend. These results suggest that popA may have experienced more heterogeneous environmental conditions that promoted greater genetic variability, while popB appears more isolated, leading to lower diversity. This pattern is consistent with the idea that populations in more variable environments tend to exhibit higher genetic diversity. Furthermore, the negative inbreeding coefficients for all populations further

support the idea that prevalent outbreeding or recent admixture are contributing to the observed genetic diversity and preventing inbreeding depression.

The observed transition-to-transversion (TS:TV) ratio of 1.42 (58.65% transitions vs. 41.35% transversions) in our study of *D. citri* deviates from the expected 2:1 ratio commonly observed in many eukaryotic genomes. This discrepancy may arise from methylation effects. In insect genomes, cytosine methylation can lead to the deamination of methylated cytosines, converting them into thymine and thus increasing the frequency of C·G to T·A transitions (Yi & Goodisman 2009). However, studies have shown that the TS:TV ratio is not universally elevated in all insect genomes, suggesting that methylation alone does not account for the observed ratio (Keller *et al.* 2007). This variability may also be influenced by nucleotide composition or other genomic characteristics that affect mutation types.

InDel analysis revealed a higher frequency of shorter insertions and deletions, with 63% of InDel sites located in exonic regions. This suggests that these mutations may be functionally significant, affecting gene expression or protein function, which could play a role in adaptation to environmental pressures. The observed higher frequency of InDels in exonic regions aligns with the hypothesis that coding sequences are under selective pressures that could affect protein-coding genes involved in crucial biological processes. Several factors may account for this observation. First, some insect genomes exhibit unique structural features, such as a higher density of repetitive elements and a greater proportion of coding sequences, which can predispose exonic regions to a higher frequency of InDels. Studies have shown that variations in genome size among insects are largely due to differences in repetitive element content, which influences InDel distribution (Cong *et al.* 2022). Second, high sequencing depth can lead to the detection of both true and artifact-induced InDels. In regions with high coverage, even minor sequencing errors, such as base miscalls or incorrect alignments, can be interpreted as InDels, potentially inflating the observed frequency in exonic regions. Lastly, exonic regions, particularly those with repetitive sequences or high GC content, can pose alignment challenges. Misalignments in these regions can lead to erroneous InDel calls, a recognized issue in InDel detection where mapping errors can result in a low signal-to-noise ratio (Challis *et al.* 2015). To mitigate these issues, we implemented rigorous quality control measures during sequencing and data processing, optimized variant calling pipelines for insect genomes, and ensured methodological transparency in our bioinformatics approaches. These steps aim to enhance the reliability of our findings and provide a comprehensive understanding of the genetic landscape of *D. citri*.

Regarding selective sweeps, the analysis combining F_{st} statistics and θ_{π} indices revealed that more candidate regions were under selection in popA than in popB and popC. This suggests that popA may have undergone more recent adaptive evolution or experienced stronger selective pressures. The GO annotations and KEGG pathway enrichment analysis of the selection sweep regions identified significant associations with cellular components like the cytosol, molecular functions such as octopamine receptor activity, and biological processes related to cytokine receptor binding. These findings emphasize the importance of signaling pathways in maintaining the fitness of *D. citri* populations. Furthermore, the KEGG pathway enrichment analysis revealed significant associations with endocrine and calcium reabsorption pathways, highlighting potential physiological mechanisms involved in adaptation to local environmental conditions or host plant interactions (Chattopadhyay *et al.* 1996). These findings are consistent with those observed in other Chinese populations, where genes involved in stress tolerance, neurotransmission, and hormonal regulation play vital roles in adaptation to changing environmental conditions, such as pesticide exposure and host plant variation (Luo & Agnarsson 2018; Tang *et al.* 2021). These insights contribute to understanding the adaptive mechanisms of *D. citri* and could inform future pest management strategies.

However, this study has some limitations. The sample size, although sufficient for an initial exploration of genetic structure, could be expanded to include more individuals and populations across different citrus-growing regions. Such an expansion would help clarify whether the observed patterns of genetic differentiation are localized to southeastern Sichuan or reflect broader regional or global trends. Additionally, this study did not incorporate environmental data such as climate, host plant composition, or agricultural practices, all of which may significantly

influence genetic structure and local adaptation. Future studies that integrate both genetic and ecological data could provide a more comprehensive understanding of how environmental factors shape the genetic makeup of *D. citri* populations.

Another area for future research involves validating the roles of the candidate genes identified in this study. While genetic markers related to stress response and endocrine regulation have been implicated, further functional genomics studies are necessary to confirm their roles in traits such as pesticide resistance and host plant adaptation. These could involve gene expression studies or targeted gene-editing techniques such as CRISPR to elucidate the functional impact of these genes on fitness and adaptation.

The findings of this study contribute significantly to the understanding of the genetic diversity and adaptive mechanisms of *D. citri* in Sichuan Province of China. This knowledge can help inform pest management strategies and potentially aid in predicting the spread of the pest in this area, thereby assisting in the implementation of more effective and sustainable integrated pest management strategies.

Acknowledgements

We thank the anonymous reviewers for valuable comments.

References

Ajene IJ, Khamis FM, van Asch B, Pietersen G, Seid N, Wairimu AW, Ombura FL, Akutse KS, Sétamou M, Subramanian S, Mohammed S & Ekesi S 2022: Genetic diversity of *Diaphorina citri* (Hemiptera: Liviidae) unravels phylogeographic structure and invasion history of eastern African populations. *Ecology and Evolution*, 12 [e9090]: 1–15. https://doi.org/10.1002/ece3.9090

Alexander DH, Novembre J & Lange K 2009: Fast model-based estimation of ancestry in unrelated individuals. *Genome Research*, 19: 1655–1664. https://doi.org/10.1101/gr.094052.109

Catchen J, Hohenlohe PA, Bassham S, Amores A & Cresko WA 2013: Stacks: An analysis tool set for population genomics. *Molecular Ecology*, 22: 3124–3140. https://doi.org/10.1111/mec.12354

Challis D, Antunes L, Garrison E, Banks E, Evani US, Muzny D, Poplin R, Gibbs RA, Marth G & Yu F 2015: The distribution and mutagenesis of short coding INDELs from 1,128 whole exomes. *BMC Genomics*, 16: 1–9. https://doi.org/10.1186/s12864-015-1333-7

Chattopadhyay N, Mithal A & Brown EM 1996: The calcium-sensing receptor: a window into the physiology and pathophysiology of mineral ion metabolism. *Endocrine Reviews*, 17: 289–307. https://doi.org/10.1210/edrv-17-4-289

Chen S, Zhou Y, Chen Y & Gu J 2018: fastp: an ultra-fast all-in-one FASTQ preprocessor. *Bioinformatics*, 34: i884–i890. https://doi.org/10.1093/bioinformatics/bty560

Cong Y, Ye X, Mei Y, He K & Li F 2022: Transposons and non-coding regions drive the intrafamily differences of genome size in insects. *iScience*, 25 [104873]: 1–20. https://doi.org/10.1016/j.isci.2022.104873

Deng TJ, Yang LT, Lei W, Liu LH, Liu JM & Chen Q 2024: Genetic diversity and population structure analysis of *Diaphorina citri* Kuwayama in Guangxi based on mitochondrial gene sequences. *Journal of South Agricultural Sciences*, 55 (7): 2100–2107. [邓铁军, 杨丽婷, 雷薇, 刘丽辉, 刘吉敏 & 陈琦 2024: 基于线粒体基因序列的广西柑橘木虱遗传多样性及种群结构分析. 南方农业学报, 55 (7): 2100–2107.] https://doi.org/10.3969/j.issn.2095-1191.2024.07.021

Du J, Wang Q, Shi H, Zhou C, He J & Wang X 2023: A prophage-encoded effector from *Candidatus Liberibacter asiaticus* targets ASCORBATE PEROXIDASE6 in citrus to facilitate bacterial infection. *Molecular Plant Pathology*, 24: 302–316.

https://doi.org/10.1111/mpp.13296

Fuentes A, Braswell WE, Ruiz-Arce R & Racelis A 2018: Genetic variation and population structure of *Diaphorina citri* using cytochrome oxidase I sequencing. *PLoS ONE*, 13 [e0198399]: 1–17.
https://doi.org/10.1371/journal.pone.0198399

Grafton-Cardwell EE, Stelinski LL & Stansly PA 2013: Biology and management of Asian citrus psyllid, vector of the Huanglongbing pathogens. *Annual Review of Entomology*, 58: 413–432.
https://doi.org/10.1146/annurev-ento-120811-153542

Guidolin AS, Fresia P & Consoli FL 2014: The genetic structure of an invasive pest, the Asian citrus psyllid *Diaphorina citri* (Hemiptera: Liviidae). *PLoS ONE*, 9 [e115749]: 1–17.
https://doi.org/10.1371/journal.pone.0115749

Hall DG, Richardson ML, Ammar ED & Halbert SE 2013: Asian citrus psyllid, *Diaphorina citri*, vector of citrus huanglongbing disease. *Entomologia Experimentalis et Applicata*, 146: 207–223.
https://doi.org/10.1111/eea.12025

Hill WG & Robertson A 1968: Linkage disequilibrium in finite populations. *Theoretical and Applied Genetics*, 38: 226–231.
https://doi.org/10.1007/BF01245622

Huang A, Ma J, Yang J, Chen B, Zhou J & Yi L 2024: Genetic diversity and population structure of the Asian citrus psyllid in China. *Journal of Insect Science*, 24 [2]: 1–8.
https://doi.org/10.1093/jisesa/iead120

Huang DW, Sherman BT & Lempicki RA 2009: Systematic and integrative analysis of large gene lists using DAVID bioinformatics resources. *Nature Protocols*, 4: 44–57.
https://doi.org/10.1038/nprot.2008.211

Keller I, Bensasson D & Nichols RA 2007: Transition-transversion bias is not universal: a counter example from grasshopper pseudogenes. *PLOS Genetics*, 3 [e22]: 185–191.
https://doi.org/10.1371/journal.pgen.0030022

Lashkari M, Manzari S, Sahragard A, Malagnini V, Boykin LM & Hosseini R 2014: Global genetic variation in the Asian citrus psyllid, *Diaphorina citri* (Hemiptera: Liviidae) and the endosymbiont *Wolbachia*: links between Iran and the USA detected. *Pest Management Science*, 70: 1033–1040.
https://doi.org/10.1002/ps.3643

Lewontin RC 1964: The interaction of selection and linkage. I. General considerations; heterotic models. *Genetics*, 49: 49–67.
https://doi.org/10.1093/genetics/49.1.49

Li H 2013: Aligning sequence reads, clone sequences and assembly contigs with BWA-MEM. *arXiv*, [1303.3997v2]: 1–3.

Luo Y & Agnarsson I 2018: Global mtDNA genetic structure and hypothesized invasion history of a major pest of citrus, *Diaphorina citri* (Hemiptera: Liviidae). *Ecology and Evolution*, 8: 257–265.
https://doi.org/10.1002/ece3.3680

Luo Y, Wu K, Fu D, Wang A & Xu B 2019: Population genetic structure of the Asian citrus psyllid, *Diaphorina citri* Kuwayama (Hemiptera: Liviidae) in Jiangxi. *Plant Protection*, 45: 55–59. [罗育发, 吴凯, 付丹, 王艾平 & 徐兵 2019: 江西亚洲柑橘木虱的种群遗传结构研究. 植物保护, 45 (3): 55–59.]
https://doi.org/10.16688/j.zwbh.2018234.

McKenna A, Hanna M, Banks E, Sivachenko A, Cibulskis K, Kernytsky A, Garimella K, Altshuler D, Gabriel S, Daly M & DePristo MA 2010: The Genome Analysis Toolkit: a MapReduce framework for analyzing next-generation DNA sequencing data. *Genome Research*, 20: 1297–1303.
https://doi.org/10.1101/gr.107524.110

Pérez-Valencia LI, Michel AP, Moya-Raygoza G & Rodríguez A 2019: Genetic variation and structure of *Diaphorina citri* (Hemiptera: Liviidae) in populations from México. *Annals of the Entomological Society of America*, 112: 379–387.
https://doi.org/10.1093/aesa/saz016

Pfeifer B, Wittelsbürger U, Ramos-Onsins SE & Lercher MJ 2014: PopGenome: An efficient swiss army knife for population genomic analyses in R. *Molecular Biology and Evolution*, 31: 1929–1936.

https://doi.org/10.1093/molbev/msu136

Pickrell JK & Pritchard JK 2012: Inference of population splits and mixtures from genome-wide allele frequency data. *PLoS Genetics*, 8 [e1002967]: 1–17.
https://doi.org/10.1371/journal.pgen.1002967

Price MN, Dehal PS & Arkin AP 2009: FastTree: computing large minimum evolution trees with profiles instead of a distance matrix. *Molecular Biology and Evolution*, 26: 1641–1650.
https://doi.org/10.1093/molbev/msp077

Purcell S, Neale B, Todd-Brown K, Thomas L, Ferreira MAR, Bender D, Maller J, Sklar P, de Bakker PIW, Daly MJ & Sham PC 2007: PLINK: a tool set for whole-genome association and population-based linkage analyses. *American Journal of Human Genetics*, 81: 559–575.
https://doi.org/10.1086/519795

Qasim M, Baohua W, Zou H, Lin Y, Dash CK, Bamisile BS, Hussain M, Zhiwen Z & Wang L 2018: Phylogenetic relationship and genetic diversity of citrus psyllid populations from China and Pakistan and their associated *Candidatus* bacterium. *Molecular Phylogenetics and Evolution*, 126: 173–180.
https://doi.org/10.1016/j.ympev.2018.04.028

Song Z-R, Li Y-H, Ou D, Qiu B-L & Sang W 2018: Phylogenetic analysis of *Diaphorina citri* from Southern China based on COI gene. *Subtropical Plant Science*, 47: 18–22. [宋章蓉, 李翌菡, 欧达, 邱宝利 & 桑文 2018: 基于 COI 基因的华南地区柑橘木虱系统发育研究. 亚热带植物科学, 47 (1): 18–22.]

Tang T, Zhao M, Wang P, Huang S & Fu W 2021: Control efficacy and joint toxicity of thiamethoxam mixed with spirotetramat against the Asian citrus psyllid, *Diaphorina citri* Kuwayama. *Pest Management Science*, 77: 168–176.
https://doi.org/10.1002/ps.6004

VanRaden PM 2008: Efficient methods to compute genomic predictions. *Journal of Dairy Science*, 91: 4414–4423.
https://doi.org/10.3168/jds.2007-0980

Wang K, Li M & Hakonarson H 2010: Annovar: Functional annotation of genetic variants from high-throughput sequencing data. *Nucleic Acids Research*, 38 [e164]: 1–7.
https://doi.org/10.1093/nar/gkq603

Wang Y, Xu C, Tian M, Deng X, Cen Y & He Y 2017: Genetic diversity of *Diaphorina citri* and its endosymbionts across east and south-east Asia. *Pest Management Science*, 73: 2090–2099.
https://doi.org/10.1002/ps.4582

Yang J, Lee SH, Goddard ME & Visscher PM 2011: GCTA: A tool for genome-wide complex trait analysis. *American Journal of Human Genetics*, 88: 76–82.
https://doi.org/10.1016/j.ajhg.2010.11.011

Yi SV & Goodisman MAD 2009: Computational approaches for understanding the evolution of DNA methylation in animals. *Epigenetics*, 4: 551–556.
https://doi.org/10.4161/epi.4.8.10345

Zhang C, Dong S-S, Xu J-Y, He W-M & Yang T-L 2019: PopLDdecay: a fast and effective tool for linkage disequilibrium decay analysis based on variant call format files. *Bioinformatics*, 35: 1786–1788.
https://doi.org/10.1093/bioinformatics/bty875

Zhang C, Xiong X, Liu X, Zou Z, Xin T, Wang J & Xia B 2019: *Diaphorina citri* (Hemiptera: Psylloidea) in China: two invasion routes and three transmission paths. *Journal of Economic Entomology*, 112: 1418–1427.
https://doi.org/10.1093/jee/toz046

Zheng Z, Chen J & Deng X 2018: Historical perspectives, management, and current research of citrus HLB in Guangdong Province of China, where the disease has been endemic for over a hundred years. *Phytopathology*, 108: 1224–1236.
https://doi.org/10.1094/PHYTO-07-18-0255-IA

Additional information

Author contributions: Conceptualization: H-L Liu & M Wang. Project administration: X Liu & M Wang. Resources: C-Y Yi & M Wang. Supervision: X Liu & M Wang. Visualization: C-Y Yi. Writing–original draft: H-L Liu, Y-P Wang & S Chen. Writing–review and editing: C-C Zhang & Q-D Chen. Funding acquisition: X Liu & M Wang.

Conflict of interest: The authors have declared that no competing interests exist.

Data availability: All of the data that support the findings of this study are available in the main text.

Ethical statement: No ethical statement was reported.

Funding: This research was financially supported by the Sichuan Fruit Innovation Team of National Modern Agricultural Industry Technology System (SCCXTD-2024-4), Infestation Regularity and Control Technology of Primary Pests on Characteristic Fruit of Sichuan Province (2022ZZCX018), and Enhancement of Pengan Comprehensive Experimental Station for Green Economic Crops, Sichuan Academy of Agricultural Sciences (2025-2030).

Disclaimer/Publisher's Note: The statements, opinions and data contained in all publications are solely those of the individual author(s) and contributor(s) and not of *ICE* and/or the editor(s). *ICE* and/or the editor(s) disclaim responsibility for any injury to people or property resulting from any ideas, methods, instructions or products referred to in the content.